Scaled boundary finite element method for stress intensity factor and T-stress computation

Santosh Shrestha * and Mitao Ohga **

*Member, Graduate student, Dept. of Civil & Envn. Eng., Ehime University, Bunkyo-cho 3, Matsuyama 790-8577
** Member, Dr. of Eng., Professor, Dept. of Civil & Envn. Eng., Ehime University, Bunkyo-cho 3, Matsuyama 790-8577

In this paper, scaled boundary finite element method is applied to various crack problems to demonstrate the efficiency and accuracy of the method. The fracture parameters that are not only of the inverse square root singular term - SIFs but also of the constant non-singular terms - elastic T-stress, of the stress fields near crack-tip are computed using a simple and direct formulation proposed by authors. The proposed formulations for evaluating SIFs and elastic T-stress, of the stress fields near crack-tip are derived by comparing the stress field ahead of a crack-tip with that of standard Williams' eigenfunction solution for the crack-tip. Four numerical examples for a range of crack sizes with different loading and geometry are analysed to examine the accuracy and efficiency of the method. The computed results are in remarkable agreement with available values in the literatures.

Key Words:, SIFs, T-stress, crack-tip stress field, scaled boundary finite element method

1. Introduction

The study of the stress and displacement fields near crack-tip in fracture mechanics is very important because these fields govern the fracture process that takes place at the crack-tip. Generally, a single parameter, called stress intensity factors (SIFs), has been used for years to characterize the stress and displacement fields near a crack-tip for the fracture behaviors. Recently, the elastic *T*-stress is being recognized as an important additional parameter besides the SIFs for fracture analysis and hence the accurate and efficient numerical evaluation of these parameters for cracked geometries has been receiving much attention. The *T*-stress corresponds to the second, non-singular term of William's eigenfunction expansion[1] of linear elastic stress field near a crack-tip, which is the constant stress acting parallel to the crack flank. The experimental tests conducted by Williams and Ewing[2] on mixed mode fracture showed that the inclusion of this term could improve the accuracy of the theoretical predictions of the crack initiation angle and the critical SIFs. Other studies indicated that *T*-stress has significant influence on crack growth direction, crack growth stability, crack-tip constraint and fracture toughness [3-4].

It is well known that how to model the crack is the key issue in the analyses. Since fracture parameters can only be determined analytically for a very few idealized cases, in general, numerical methods must be employed for practical problems. Among the numerical techniques, finite element method (FEM) and boundary element method (BEM) are most popular when rigorous solutions of complex inclusion problems are required. Unfortunately, these methods have some limitations and are inefficient in dealing with crack-tip problems, even within the linear elastic regime. When standard FEM is used, extremely fined meshes must be employed around the crack-tip with whole domain discretisation to capture the characteristic of singular stress fields that leads to slow convergence. In order to improve the rate of convergence, sophisticated mesh generation procedures or adaptive techniques must be employed. Hybrid crack element (HCE) method [5], singular p-version FEM [6], s-version FEM (s-FEM)[7], extended-FEM (X-FEM)[8], and partition-of-unity FEM (PUFEM) [9] are the some of the recently developed method to deal the singular stress field more accurately. BEM has some advantages over FEM since it only needs boundary discretisation of the studied problems. But BEM needs a lot of skills because in numerical implementation, one needs

fundamental solution and advanced mathematical knowledge to deal with various singular integrals. Besides, the standard FEM and BEM are based on assumed piecewise smooth functions, which do not resemble the exact solution near the singular point[10]. The scaled boundary finite element method (SBFEM), a new semi-analytical method, is emerging as an alternative approach in order to overcome the deficiencies of FEM and BEM. As will be discussed later, SBFEM can accurately compute stress and displacement field of singularities region at the crack-tip without any *a priori* assumption when the 'scaling center' lies on the crack-tip.

SBFEM was previously applied to determine stress intensity factors by Song and Wolf [11], and Deeks [12]. Song [13] applied SBFEM to determine dynamic SIFs by using super elements. All these studies have addressed only the computations of SIFs for the crack problems with simple geometries and loading condition. Recently, authors [14] applied SBFEM to compute the singular and higher order coefficients terms of crack-tip stress fields. In Ref. [14], a simple technique for evaluating coefficients of stress field near a crack-tip is proposed by comparing the stress field along the radial points ahead of the crack-tip with that of standard Williams' eigenfunction expansion of the linear elastic stress field at the crack-tip. However, authors also considered only simple benchmark problems to demonstrate the effectiveness of the proposed method.

The main purpose of this paper is to apply the SBFEM for computing the fracture parameters, not only the inverse square root singular term - SIFs but also of the constant non-singular terms - elastic T-stress, of the stress fields near crack-tip of various crack problems with complex geometry and loading. In this paper, the technique proposed by authors[14] is applied to evaluate the fracture parameters. The proposed SBFEM formulation can be applied directly as well as independently to evaluate T-stress and SIFs for various cracks from semi-analytical solution without any post-processing. Moreover, in this proposed method, the so-called scaling center is placed at crack-tip that omits the discretisation of the straight crack faces and near crack-tip, which is the notorious difficulty encountered in other methods.

2. Scaled boundary finite element method

The scaled boundary finite element method is a new semi-analytical fundamental solution-less BEM based on FEM[15]. In this method, the partial differential equation of a variety of linear problems is transformed into ordinary differential equations. Then, these ordinary differential equations are solved analytically in radial direction and the coefficients of these equations are determined by the finite element approximation in the circumferential directions. The virtual work derivations of the stress and displacement fields in the method are presented in detail in Ref. [16] but are summarized here for convenience as follows

Governing equations of elastostatics

For two-dimensional elastostatics problems, the strains $\{\varepsilon(x,y)\}$ related to the displacement $\{u(x, y)\}$ by

$$\{\varepsilon(x,y)\} = \begin{Bmatrix} \varepsilon_x \\ \varepsilon_y \\ \gamma_{xy} \end{Bmatrix} = \begin{bmatrix} \partial/\partial x & 0 \\ 0 & \partial/\partial y \\ \partial/\partial y & \partial/\partial x \end{bmatrix} \begin{Bmatrix} u_x \\ u_y \end{Bmatrix} \quad (1)$$
$$= [L]\{u(x,y)\}$$

where $[L]$ is linear differential operator.

And the stresses $\{\sigma(x,y)\}=[\sigma_x, \sigma_y, \tau_{xy}]^T$ are given by

$$\{\sigma(x,y)\} = [D]\{\varepsilon(x,y)\} = [D][L]\{u(x,y)\} \quad (2)$$

with the elasticity matrix $[D]$

In no body load case, the internal equilibrium in elastostatics leads to the differential equation

$$[L]^T\{\sigma(x,y)\} = 0 \quad (3)$$

which must be satisfied at every point within the domain.

Scaled boundary coordinate system

In this method, a coordinate system consists of a radial direction (ξ) and a local circumferential direction (η) is introduced (Fig. 1). The radial coordinate is defined to be zero at 'scaling center', and to have unit value on the domain boundary. The circumferential coordinate measures the distance anticlockwise around the boundary. The coordinate system is termed the scaled boundary coordinate system, and related to Cartesian coordinate by

$$x = x_0 + \xi\, x(\eta) \quad (4a)$$

$$y = y_0 + \xi\, y(\eta) \quad (4b)$$

where $x(\eta)$ and $y(\eta)$ are the functions describing the variation of the boundary in x and y directions as functions of η.

Applying standard procedures to transform the geometry from Cartesian co-ordinates to the scaled boundary co-ordinates defined in above Eq. (4), the linear operator in Eq. (1) can be written in the co-ordinate ξ, η as

$$[L] = [b^1(\eta)]\frac{\partial}{\partial \xi} + \frac{1}{\xi}[b^2(\eta)]\frac{\partial}{\partial \eta} \quad (5)$$

where $[b^1(\eta)]$ and $[b^2(\eta)]$ depend only on the geometry of the boundary.

Displacement function

The displacements at any point in the domain defined by scaled boundary coordinates (ξ, η) can be expressed in the form:

$$\{u(\xi,\eta)\} = \sum_{i=1}^{n} N_i(\eta)\{u_i(\xi)\} = [N(\eta)]\{u(\xi)\} \quad (6)$$

which represents a discretisation of the boundary only.

Substituting Eqs. (5) and (6) in Eq. (3) lead to the approximate stresses in the co-ordinate ξ, η as

$$\{\sigma(\xi,\eta)\} = [D][B^1(\eta)]\{u(\xi)\}_{,\xi} + \frac{1}{\xi}[D][B^2(\eta)]\{u(\xi)\} \quad (7)$$

where

$$[B^1(\eta)] = [b^1(\eta)][N(\eta)]$$
$$[B^2(\eta)] = [b^2(\eta)][N(\eta)]_{,\eta} \quad (8)$$

These results can be used in the virtual work equation to solve for the radial displacements.

Scaled boundary finite element equation

The virtual work statement is applied to introduce the equilibrium. When the domain is subjected to a set of boundary tractions $\{t\}$, the virtual work statement is

$$\int_V \{\delta\varepsilon\}^T\{\sigma\}dV = \int_S \{\delta u\}^T\{t\}ds \quad (9)$$

Performing integrals over the domain and then a series of mathematical manipulations, the virtual work statement is satisfied for all virtual displacements $\{\delta u(\xi)\}$ when

$$[E^0]\xi^2\{u(\xi)\}_{\xi\xi} + [[E^0] + [E^1]^T - [E^1]]\xi\{u(\xi)\}_{\xi} - [E^2]\{u(\xi)\} = 0 \quad (10)$$

where the coefficient matrices

$$[E^0] = \int_{-1}^{1}[B^1]^T[D][B^1]|J|d\eta \quad (11a)$$

$$[E^1] = \int_{-1}^{1}[B^2]^T[D][B^1]|J|d\eta \quad (11b)$$

$$[E^2] = \int_{-1}^{1}[B^2]^T[D][B^2]|J|d\eta \quad (11c)$$

are independent of ξ. The integrals of these $[E^0]$, $[E^1]$, and $[E^2]$ are evaluated using *Gaussian quadrature*. Eq. (10) is a standard ordinary differential equation for the displacements $u(\xi)$ with the dimensionless radial coordinate ξ as the independent variable.

Solution procedures

By inspection, solution to the set of Euler-Cauchy differential equation represented by Eq. (10) must be of the form

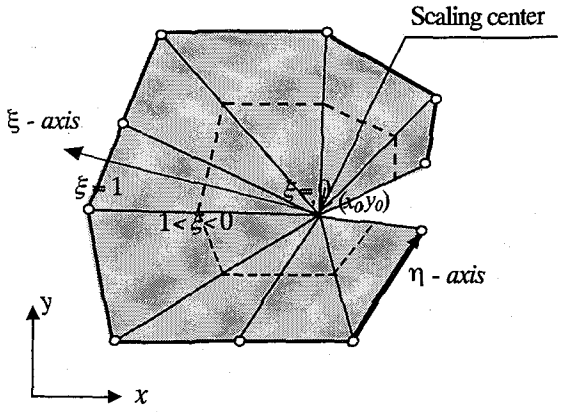

Fig 1 Scaled boundary coordinate system

$$\{u(\xi)\} = \sum_{i=1}^{n} c_i\xi^{-\lambda_i}\{\phi_i\} \quad (12a)$$

where the exponents λ_i and vectors $\{\phi_i\}$ are interpreted as a radial scaling factor and a displacement modes shapes. The integration constants c_i represent the contribution of each mode to the solution, and are dependent on the boundary conditions.

The displacements for each mode from Eq. (12a) can be written as

$$\{u(\xi,\eta)\} = \xi^{-\lambda}\{\phi\} \quad (12b)$$

Now substituting Eq. (12b) and its derivations into Eq. (10) and then simplifying yields the quadratic eigenproblem.

$$[\lambda^2[E^0] - \lambda[[E^1]^T - [E^1]] - [E^2]]\{\phi\} = \{0\} \quad (13)$$

This eigenproblem can be solved using standard techniques, yielding $2n$ displacement modes, where n is the number of nodes used in boundary discretisation, and hence is also the size of the coefficient matrices.

Bounded problems can be represented conveniently by taking $0 \le \xi \le 1$. For such problems, only n modes with negative real component of λ lead to finite displacements at scaling center. This subset of n nodes is denoted by $[\Phi_1]$. For any set of boundary node displacements, u, the integration constants are

$$\{c\} = [\Phi_1]^{-1}\{u\} \quad (14)$$

The displacement fields can be obtained using

$$\{u(\xi,\eta)\} = [N(\eta)]\sum_{i=1}^{n} c_i\xi^{-\lambda_i}\{\phi_i\} \quad (15)$$

and the stress field

$$\{\sigma(\xi,\eta)\} = [D]\sum_{i=1}^{n}[c_i\xi^{-\lambda_i-1}[-\lambda_i[B^1(\eta)] + [B^2(\eta)]]\{\phi_i\}] \quad (16)$$

Eqs. (15) and (16) are, respectively, the semi-analytical solutions for displacement and stress fields inside the domain.

3. Determination of SIFs and elastic T-stress

Two fracture parameters – SIF and T-stress

The Williams' eigenfunction expansion[1] for crack-tip stress fields in any linear elastic body is given by a series of the form

$$\sigma_{ij}(r,\theta) = A_1 r^{-1/2} f_{ij}^{(1)}(\theta) + A_2 r^{o} f_{ij}^{(2)}(\theta) + \ldots\ldots \quad (17)$$

where (r, θ) are the local polar coordinates with the origin at the crack-tip, as shown in Fig. 2, the coefficients A_1, A_2 embodies SIFs and T-stress respectively whose values vary with applied load and geometry of the cracked body and $f_{ij}(\theta)$ is a function describing the angular variation of the stress field. The first term is singular at the crack-tip, and is controlled by the elastic SIF. The second term is referred to as a constant non-singular components and vanishes for pure mode II.

According to Ref. [17], the asymptotic stress field for Mode I can be written as

$$\begin{Bmatrix}\sigma_x\\ \sigma_y\\ \tau_{xy}\end{Bmatrix} = \frac{K_I}{\sqrt{2\pi r}}\cos\left(\frac{\theta}{2}\right)\begin{Bmatrix}1-\sin\left(\frac{\theta}{2}\right)\sin\left(\frac{3\theta}{2}\right)\\ \sin\left(\frac{\theta}{2}\right)\cos\left(\frac{3\theta}{2}\right)\\ 1+\sin\left(\frac{\theta}{2}\right)\sin\left(\frac{\theta}{2}\right)\end{Bmatrix} + \begin{Bmatrix}T\\0\\0\end{Bmatrix} + \sum_{n=3}^{\infty} A_n r^{n-1/2}\begin{Bmatrix}f_x^{(n)}(\theta)\\ f_y^{(n)}(\theta)\\ f_{xy}^{(n)}(\theta)\end{Bmatrix} \quad (18)$$

To normalize the effect of T-stress relative to the SIF in mode I, Leevers and Radon [18] proposed a dimensionless parameter called the biaxiality ratio B, as

$$B = T\frac{\sqrt{\pi a}}{K_I} \quad (19)$$

where a is the length of the crack. The dependence on geometrical configurations can be best indicated by the biaxiality parameter B.

SBFEM formulation for fracture parameters

In the numerical SBFEM analysis, let us consider the so-called 'scaling center' at the crack-tip, as shown in the Fig. 2 and the stress field along the radial direction emanating from the crack-tip where the stress singularity occurs are analytically calculated to approximate the crack-tip along the line of propagation of the crack. In this consideration, only the boundaries, but not the straight crack faces and faces passing through the crack-tip, are discretised,

Now the stress field Eq. (16) can be expanded as

$$\sigma(\xi,\eta) = A_1\xi^{-1/2} + A_2\xi^0 + A_3\xi^{1/2} + \ldots + A_n\xi^{n/2-1} = \sum_{i=1}^{n} A_i\xi^{i/2-1} \quad (20)$$

where the coefficients $A_i = c_i\{\hat{\sigma}(\eta)\}_i$ that depend only on the circumferential coordinate η, and are constants for a given radial direction of a given element.

The stress components $\hat{\sigma}(\eta)$ are

$$\{\hat{\sigma}(\eta)\} = \{\hat{\sigma}_x, \hat{\sigma}_y, \hat{\sigma}_{xy}\}^T = [D][-\lambda[B^1(\eta)] + [B^2(\eta)]]\{\phi\} \quad (21)$$

and the power of ξ is

$$\lambda_i = \frac{i}{2} \qquad \forall\ i = 1,2,3,\ldots,n \quad (22)$$

For a given radial direction emanating from the crack-tip and inclined at an angle θ to the global x-axis as shown in Fig. 2, the following relationships are obtained from Eq. (4) as

$$r = r(\xi,\eta) = \xi\hat{r} \quad (23)$$

where $\hat{r} = r(\eta) = \sqrt{x(\eta)^2 + y(\eta)^2}$ are the radial distances of the boundary nodes from scaling center, and r is a distance measured from the crack-tip along the ray. The angle θ and the distance $\hat{r}$ are constants for a given radial direction of a given element.

After substituting Eq. (23), Eq. (20) becomes

$$\sigma(\xi,\eta) = \{A_1\hat{r}^{1/2}\}r^{-1/2} + \{A_2 r^0\}r^0 + \{A_3\hat{r}^{-1/2}\}r^{1/2} + \ldots + A_n\hat{r}^{n/2-1}\}r^{n/2-1} = \sum_{i=0}^{n} A_i\hat{r}^{-i/2-1}r^{i/2-1} \quad (24)$$

Eq. (24) is similar to Williams' expansion of the stress field, Eq. (17) at $\theta = 0$. Thus, the stress intensity factors and T-stress can be computed by equating the coefficients of first and second terms with –1/2 and 0 powers of r of Eqs. (24) and (18) as follows.

Stress intensity factor for mode I is

$$K_I = c(\hat{\sigma}_y)\sqrt{2\pi\hat{r}} \quad (25)$$

T-stress is

$$T = c(\hat{\sigma}_x) \quad (26)$$

These equations indicate that the SIFs, T-stress of the Williams' series can be directly calculated from SBFEM.

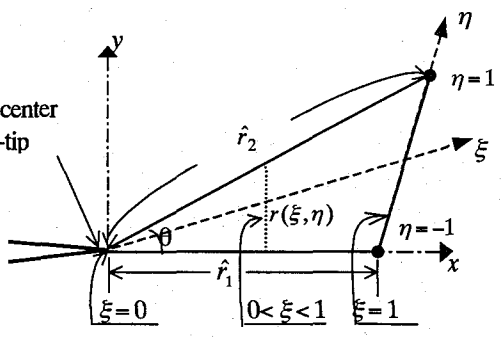

Fig. 2 SBFEM element with different coordinates

4. Numerical Examples

In this section, the proposed SBFEM formulation was applied to exacting fracture parameters, SIFs and T-stress, of a crack specimen under different loading and geometric condition. The following four fracture specimens were simulated.

i) Double edge-cracked tension (DECT) specimen,
ii) Center crack circular plate (CCCP) specimen
iii) Three point bending cracked (TPBC) specimen, and
iv) Square hole cracked plate (SHCP) specimen.

The analyses were carried out using plane strain condition with Young's modulus E = 1.0 and Poisson's ratio ν = 0.3. Unit thickness was assumed for all the specimens. Only a half of TPBC specimen and quarter of DECT, CCCP and SHCP specimen (hatched portions in schematic diagrams) were modeled by virtue of symmetry. The discretizations employed in this study consisted of three-node iso-parametric quadratic line elements on the boundary as in Ref. [14]. The scaling center was placed at the crack-tip in SBFEM mesh and, therefore, the straight crack face and the face ahead of the crack-tip were not discretised.

4.1 Double edge cracked tension (DECT) specimen

In the first example, a rectangular panel with a double edge crack under uniaxial tension loading σ_0 at top and bottom was considered. The schematic diagram of the problem is presented in Fig. 3 (*a*), where H and W are plate dimensions and a is the crack length. The problem was analysed with an aspect ratio i.e., H/W = 12. The applied load was σ_0 = 1 with its units consistent with that of E. The analysis was carried out with four different refined meshes - coarse with 22 degree of freedoms (DOFs), medium with 42 DOFs, fine with 82 and very fine with 162 DOFs, by doubling the number of elements. The errors of normalized SIFs computed from these meshes for a/W = 0.5 were 19.78, 2.86, 1.27 and 0.68% respectively. The medium mesh discretisation for H/W = 3 is given by Fig. 3 (b).

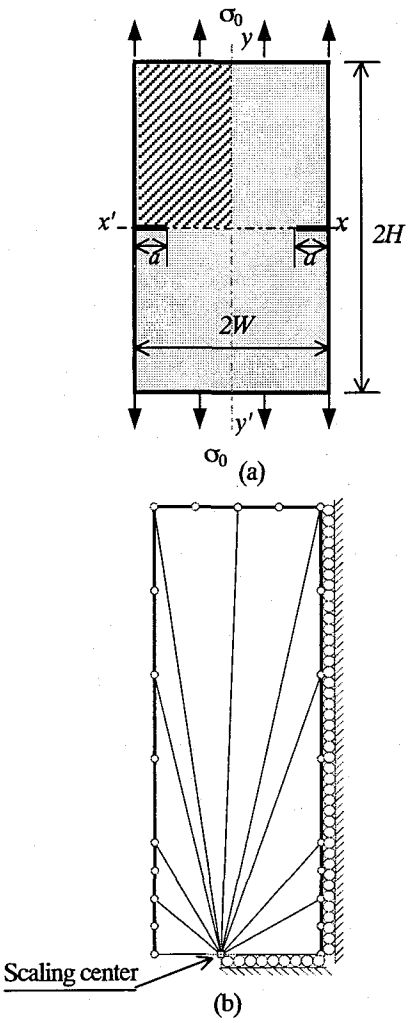

Fig. 3 (a) Schematic diagram and (b) a typical SBFEM mesh for DECT problem

Table 1 Comparison of computed SBFEM results for DECT (H/W = 12)

a/W	Sources	T/σ_0	B	$K_I/\sigma_0(\pi a)^{1/2}$
0.3	SBFEM (Present)	-0.5329	-0.4813	1.107
	SGBEM [17]	-0.5326	-0.4780	1.114
	Kim & Paulino [19]	-0.5384	-0.4444	1.212
	Fett [20]	-0.5319	-0.4720	-
0.5	SBFEM (Present)	-0.5532	-0.4765	1.161
	SGBEM [17]	-0.5521	-0.4725	1.169
	Kim & Paulino [19]	-0.5597	-0.4454	1.257
	Fett [20]	-0.5216	-0.4396	-

The results of normalized SIFs, $K_I/\sigma_0(\pi a)^{1/2}$, normalized T-stress, T/σ_0, and biaxiality ratio obtained by using Eqs. (25), (26) and (19) from very fine mesh with H/W = 12 are presented in Table 1. For H/W =12 case, the computed SBFEM results are compared with the results from Refs. [17], [19], [20]. These comparison shows that SBFEM results are in good agreement with the corresponding reference results.

4.2 Center crack circular plate problem

Second example is considered a center crack circular plate

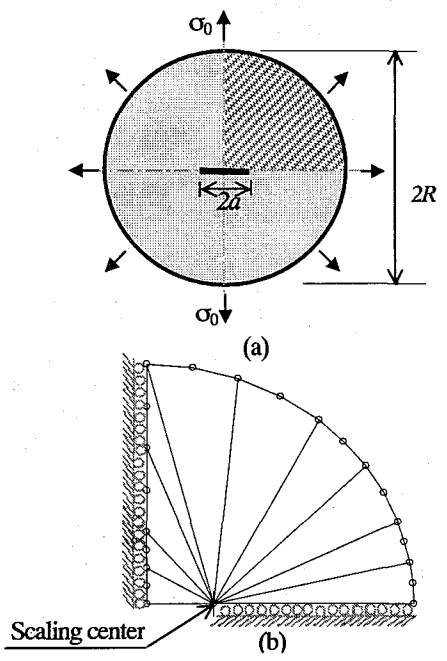

Fig. 4 (a) Schematic diagram and (b) a typical SBFEM mesh for CCCP problem

Table 2 Comparison of computed SBFEM results of normalized T-stress, T/σ_0, for CCCP

	a/R				
	0.2	0.3	0.4	0.5	0.6
Present	-0.066	-0.1705	-0.290	-0.448	-0.672
Fett [20]	-0.08	-0.171	-0.293	-0.457	-0.688
% Diff	17.13	0.29	1.02	1.97	2.33

(CCCP) with a uniform radial tension σ_0 as shown in Fig 4 (a). The problem was also analyzed with four different meshes with 5, 10, 20 and 40 elements with 22,42, 82 and 162 DOFs. The error percentages of normalized T-stress computed from these meshes for a/R = 0.3 were 16.8, 5.02, 1.36 and 0.29 % respectively. The medium mesh configuration of the problem to compute the T-stress is as shown in Fig. 4 (b). The problem was analyzed to evaluate the T-stress for varies crack length. The relative crack size, a/R, was varied from 0.2 to 0.6.

The computed results of T-stress normalized by applied stress, T/σ_0 from very fine meshes are presented in Table 2. These SBFEM results are compared with the values presented in Ref. [16]. The comparison shows that SBFEM results are in agreement with the reference values with 2 percentage deviations except for a/R = 0.2 case.

4.3 Three point bending cracked problem

Third example is the analysis of three point bending beam with single edge crack at the middle. The schematic diagram and a typical SBFEM model used for analysis are given in Fig. 5, where L and D are the span and depth of beam respectively and a is the crack length. The applied point load per unit thickness was P = 1 unit at middle as shown in Fig 5 (a). The problem was analysed to compute the SIF and T-stress with span to depth ratio L/D = 4. The relative crack length, a/D, was varied from 0.1 to 0.7, and D was taken to be 4 unit in the numerical computation.

The stress in the specimen σ_0 is defined as

$$\sigma_0 = \frac{6M}{D^2} \tag{27}$$

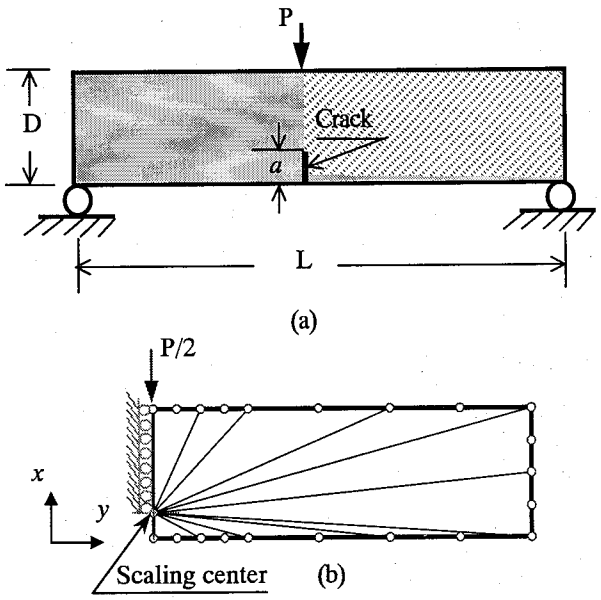

Fig. 5 (a) Schematic diagram and (b) analysis model of three point bending cracked problem

where M is the bending moment per unit thickness in the central cross section which is equal to $PL/4$ for pure bending case.

The computed results of the normalized SIFs, $K_I/\sigma_0(\pi a)^{1/2}$, and the normalized T-stress, T/σ_0, are presented in Table 3. These SBFEM results of the normalized SIFs are compared with that of HCE method from Ref. [5] and the results obtained by Guinea et al. [21], while the computed normalized T –stress are compared with the results obtained by Levers and Radon [18] and HCE method from Ref. [5]. The comparison shows that SBFEM results are in an excellent agreement with the literatures data.

4.4 Square hole cracked square specimen

The analysis of stress intensity factors in a rectangular plate with cracks emanating from a sharp-cornered square hole under biaxial loading was considered as a complex crack problem in this paper. The configuration is as shown in Fig. 6 (a). A typical SBFEM model with boundary conditions is as shown in Fig. 6 (b) and the parameter used for analysis are as following.

Table 3 Comparison of computed SBFEM results of normalized SIFs and normalized T-stress.

	Normalized SIF			Normalized T-stress		
a/D	Present	HCE [5]	Ref.[21]	Present	HCE [5]	Ref.[18]
0.15	0.264600	0.265517	0.268	-0.28800	-0.28933	-
0.2	0.309067	0.308833	0.312	-0.23527	-0.23553	-0.285
0.3	0.402717	0.402167	0.405	-0.12920	-0.12933	-0.12
0.4	0.523167	0.523283	0.527	-0.00433	-0.00367	0.02
0.5	0.701967	0.701947	0.706	0.17493	0.177867	0.18
0.6	0.994367	0.994367	1.000	0.48587	0.489133	0.38

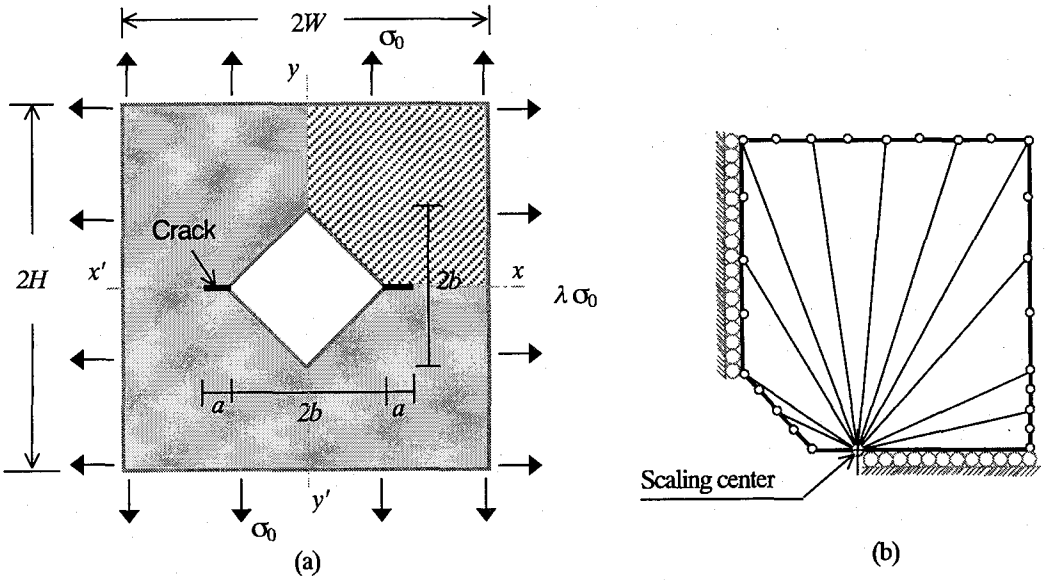

Fig. 6 (a) Schematic diagram and (b) analysis model of square hole cracked square plate

Table 4 Comparison of computed SBFEM results of normalized SIFs

	λ = 0			λ = 1			λ = −1		
a/W	Present	BEM [22]	Error %	Present	BEM [22]	Error %	Present	BEM [22]	Error %
0.30	1.2518	1.2743	1.77	0.9793	0.9983	1.90	1.5244	1.5503	1.67
0.35	1.3199	1.3222	0.17	1.0852	1.0911	0.54	1.5547	1.5533	-0.09
0.40	1.3742	1.3743	0.01	1.1677	1.1741	0.55	1.5806	1.5745	-0.39
0.50	1.5041	1.5021	-0.13	1.3319	1.3401	0.61	1.6764	1.6642	-0.73
0.60	1.6664	1.6622	-0.25	1.5155	1.5247	0.60	1.8172	1.7997	-0.97
0.70	1.8716	1.8657	-0.32	1.7400	1.7509	0.62	2.0031	1.9805	-1.14
0.80	2.1714	2.1681	-0.15	2.0634	2.0807	0.83	2.2793	2.2555	-1.06
0.85	2.4098	2.4148	0.21	2.3170	2.3443	1.16	2.5027	2.4853	-0.70
0.90	2.8072	2.8337	0.94	2.7328	2.7841	1.84	2.8817	2.8833	0.06

Plate dimension $H = W = 8$,
Dimension of square hole, b = 1,
Applied stress, $\sigma_0 = 1$,
Load factor, $\lambda = 0, 1, -1$, (Fig. 6(a)), and
Material properties, $E = 1$ and $\nu = 0.25$
All the units are consistent with the unit of E.

The problem was analysed by three different discretizations of 6, 12 and 24 elements with 26, 50, 98 DOFs respectively. The error percentages of normalized SIFs computed from these meshes for $a/W = 0.4$ were 4.5, 1.9 and 0.39 % respectively. The estimated results of fine mesh (98 DOFs) are summarized in Table 4, for various configurations of crack. To verify the accuracy and efficiency of SBFEM, the normalized SIFs that were evaluated by present SBFEM formulation are compared with those of reference solution from Ref. [22]; Ref.[22] uses BEM, which consists of crack-tip hybrid displacement discontinuity elements. All the cases that are given in Table 4 are in good agreement with the reference solutions with less than 2% deviation. Fig. 7 presents the comparative graph of the computed results with literatures (BEM) values.

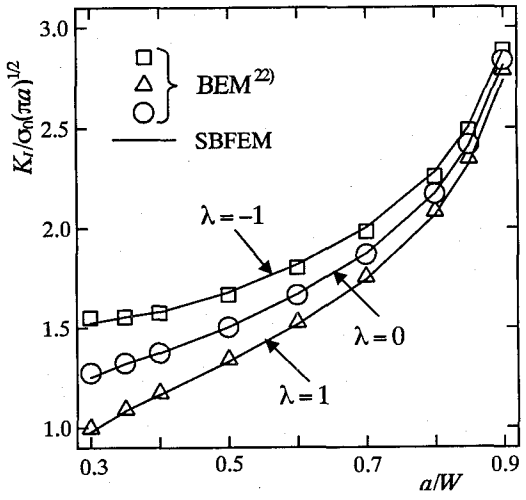

Fig. 7 Comparison of normalized SIFs results

5. Conclusion

In this paper, scaled boundary finite element method was applied to various crack problems to demonstrate the efficiency and accuracy of the method. The fracture parameters that are not only of the inverse square root singular term - SIFs but also of the constant non-singular terms - elastic T-stress, of the stress fields near crack-tip were computed using a simple and direct formulation proposed by authors. Using the proposed formulation, SIFs and T-stress for a crack can be evaluated directly by comparing the classical linear elastic field solution in the vicinity of a crack-tip to that of SBFEM after power series expansion. The accuracy of these formulations were examined with four different example problems for a range of crack sizes, loading and geometry and compared with the available solution in literatures. It can be seen that the numerical results obtained by the SBFEM formulations are in remarkable agreement with the corresponding ones in the literature for simple and complex crack problems. Based on the results of the study it can be confirmed that the proposed numerical method can be applied to crack problems more easily with relatively coarse and simple model than other computational methods for more complex crack problems.

This paper dealt with straight crack problems because of its unique advantage that omits the discretisation of the straight crack faces and face ahead of crack. The proposed method can be applied into more complex crack problems such as curved crack and concaved domain problems. To analysis these complex problem, sub –structuring with more than one scaling center is required due to one of the restrictions of SBFEM that the entire domain boundary must be visible from scaling-center.

References

1) Williams M. L. On the stress distribution at the base of a stationary crack, *J Appl Mech, ASME*, 24, pp109-14, 1957.
2) William, J.G. and Ewing, P. D. Fracture under complex stress – the angled crack problem. *Int. J. of Fracture*, 8, pp 444 - 446, 1972.
3) Du Z. Z. and Hancock J.W., The effect of non-singular stresses on crack-tip constraint. *J Mech Phys Solids*, 39, pp 555-67, 1991
4) Dyskin, A.V., Crack growth criteria incorporating non-singular stresses: Size effects in apparent fracture toughness, *Int. J. of Fracture*, 83, pp 191-206, 1997.
5) Karihaloo, B. L. and Xias, Q. Z., Higher order terms of the crack tip asymptotic field for a notched three-point bend beam. *Int. J. of Fracture*, 112, pp 111-128, 2001.
6) Rahaulkumar, P., Saigal, S. and Yunus, S., Singular p-version finite elements for stress intensity factor computations, *Int. J. Num. Meth. Engg.*, 40, pp 1091-1114, 1997.
7) Hiroshi O., Sayaka E. and Masanori K., On fracture analysis using an element overlay technique, *Engineering Fracture Mechanics*, 68, pp 1609-1630, 2005.
8) Nagashima, T, Omoto, Y. and Tani, S., Stress intensity factor analysis of interface cracks using X-FEM, *Int. J. Num. Meth. Engg.*, 56, pp 1151-1173, 2003.
9) Fan S.C., Liu X., Lee C.K., Enriched partition-of-unity finite element method for stress intensity factors at crack tips, *Computers and Structures* 82 pp 445-461, 2004.
10) Oh H. S., Babuska I., The *p*-version of the finite element method for the elliptic boundary value problems with interfaces. *Computer Methods in Applied Mechanics and Engineering*. 97, 211-231, 1992.
11) Song, C., Wolf J. P., Semi-analytical representation of stress singularity as occurring in cracks in anisotropic multi-materials with the scaled boundary finite-element method. *Computers and Structures*, 80, pp 183-197, 2002.
12) Deeks, A. J., Calculation of stress-intensity factors using the scaled boundary finite-element method. *Proc. Int. Conf. Struct. Integrity and Fracture*, Perth, pp 3-8, 2002.
13) Song C., A super-element for crack analysis in the time domain. *Int. J. Num. Meth. Engg*, 61, pp 1332-57, 2004.
14) Shrestha, S. and Ohga, M. An efficient method for computation of singular and higher order terms of a crack-tip stress field, *J Appl Mech, JSCE*, 8, pp. 171-178, 2005.
15) Wolf J.P., *The Scaled Boundary Finite Element Method*: John Wiley & Sons Ltd, 2003.
16) Deeks. A. J. and Wolf, J.P., A virtual work derivation of the scaled boundary finite element method for elastostatic, *Computational Mechanics*, 28, pp 489-509, 2002.
17) Sutradhar, A. and Paulino, G. H., Symmetric Galerkin boundary finite element computation of T-stress and SIFs for mixed-mode cracks by the interaction in integral method, *Engineering Analysis with Boundary Elements.* 28, pp 1335–1350, 2004.
18) Leevers, P.S. and Radon, J.C., Inherent stress biaxiality in various fracture specimen geometries, *Int. J. of Fracture* 19, 311▪325,1982.
19) Kim J-H.and Paulino, G. H. , A new approach to compute T-stress in functionally graded materials by means of the interaction integral method. *Engineering Fracture Mechanics* 71(13–14), pp. 1907–1950, 2004.
20) Fett T., T-stresses in rectangular plates and circular disks. *Engineering Fracture Mechanics*, 60, pp 631-652, 1998.
21) Guinea, G.V., Pastor, J.Y., Planas, J. and Elices, M. , Stress intensity factor, compliance and CMOD for a general three-point-bend beam. *International Journal of Fracture* 89, pp.103 –116,1998
22) Yan X., A numerical analysis of cracks emanating from a square hole in a rectangular plate under biaxial loads, *Engineering Fracture Mechanics*, 71, pp 1612-1623, 2004.

(Received September 10, 2005)